

SPS Induction Plasma Synthesized ZrB₂ Coatings for the Aluminium Industry

Marie-Claude Fournier¹, James Aluha¹, Faranak Barandehfard¹, Kossi Béré¹, Pierre-Olivier Langlois^{1,2}, and François Gitzhofer^{1*}

¹Department of Chemical & Biotechnological Engineering, Université de Sherbrooke, Sherbrooke, QC, J1K 2R1, Canada

²Pyrotek Inc. 4125 Rue de la Garlock, Sherbrooke, QC, J1L 1W9, Canada

Abstract: This work reports on ZrB₂-based coatings that were deposited on metallic substrates through thermal plasma technology. As a preliminary study, the effect of suspension liquids and deposition parameters evaluated the coating quality. Characterization of the materials by Microscopic imaging (SEM) coupled with X-ray elemental mapping showed uniform phase dispersion. X-ray diffraction (XRD) revealed the presence of ZrB₂ as the target phase in the coatings, and free carbon was not detected in any case.

Keywords: ZrB₂, corrosion resistance, coating, metal, SPS, induction plasma technology

1. Introduction

Zirconium diborides is an ultra-high temperature ceramic (UHTC) with an extremely high melting point (3247 ±18°C) [1]. ZrB₂ is a very interesting electrical conductor ceramic material with applications in the field of nuclear and aerospace industries. In addition, ZrB₂ has a great chemical inertness against molten aluminum-magnesium alloy. ZrB₂ resists corrosion with liquid aluminum alloys at a temperature of 700°C [2] and has excellent mechanical properties at this temperature. There has been interest in applying such coatings for industrial applications in order to extend material life and improve the process efficiency when protecting metallic parts in contact with liquid aluminum alloys.

Coatings are indeed commonly applied to protect functional components of systems working under corrosive environments. ZrB₂ coated stainless steel prepared by electro-deposition have demonstrated pronounced corrosion resistance to aluminum attacks at a temperature of 850°C compared to the uncoated substrate [3]. The absence of reactions of ZrB₂ in contact with aluminum-magnesium alloy was predicted using FactSage thermodynamic software [4], which showed that this ceramic material is quite stable in these conditions as seen in **Figure 1**.

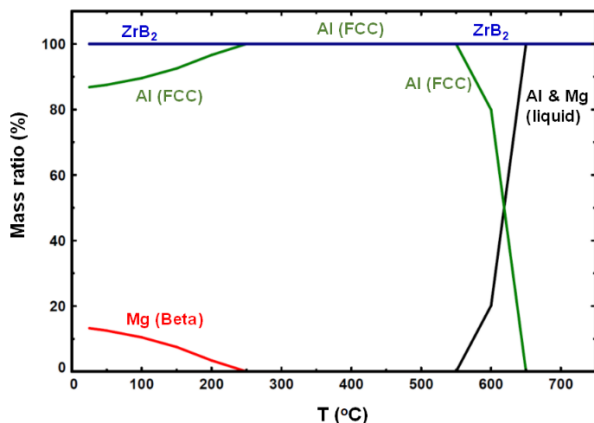
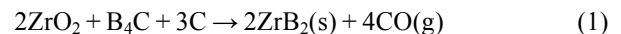


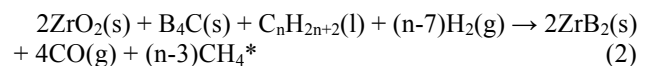
Fig. 1. FactSage plot indicating the stability of ZrB₂ in molten Al-Mg alloy.

The microstructure and phase composition of coatings formed through plasma reactive spraying of ZrO₂ and B₄C mixed powders have been studied previously using atmospheric DC plasma technology with a coating being a composite of ZrO₂ and ZrB₂ [5]. The synthesis of ZrB₂ powders by boro- and carbo-thermal reduction has also been examined [6]. Analysis by FactSage indicated that ZrO₂ can be completely reduced to ZrB₂ using an excess of B₄C in the feedstock, if the temperature is kept between 1100 and 2100°C. The selection of SPS technology in this work is to create an easy delivery method of the carbon feedstock for the chemical reaction shown in Equation (1) by using the suspension liquid as a carrier for the powders.

The present study investigates the effect of suspension liquid addition on the microstructure development and phase evolution during suspension plasma synthesis of ZrB₂ and the chosen reaction is represented by Equation (1), thus:



The composition of the suspension was theoretically determined by modelling using FactSage software and showed that the reaction between ZrO₂ and B₄C produces ZrB₂ but Zr-carbides can only be generated if the stoichiometry is not respected during plasma synthesis. The ZrO₂ and B₄C powders suspended in various suspension liquids (see **Table 1**) were plasma sprayed on a metallic substrate. The combined reactions between the powder precursors and the suspension liquid were prepared by the following reaction, with methane (CH₄*) representing the possible major by products from the decomposition of the hydrocarbons (mineral oil):



The interest in suspension plasma spraying (SPS) for the ZrB₂ deposition arises due to the flexibility in the precursors nature and composition and also in the possibility of achieving finer microstructures by spraying even nanopowders in the suspension or by changing

continuously the deposit composition [7]. The SPS system consists of a plasma reactor and an atomization probe (ref. Xi fabricated in-house at Université de Sherbrooke) thereby allowing the precursors to be injected axially [7], into a PL-50 induction plasma torch [8], which is equipped with a supersonic nozzle.

The main goal of this investigation is to protect metallic substrates against the attack of molten aluminum using a ZrB₂-based coating. The quality of the coating, its microstructure and phases obtained during the plasma deposition are currently under evaluation in terms of compactness and robustness. Testing the resistance of the coatings to the attack of molten Al-Mg alloy will follow. Preliminary tests involving sample characterization by Microscopy (SEM coupled by EDX), (X-ray diffraction (XRD) analyses and adhesion of the coating using ultrasonic bath have been conducted.

2. Experimental Methods

The SPS system operates with an induction plasma torch at 3.2 MHz alongside other system parameters, using a PL-50 [Tekna Plasma system] induction plasma torch equipped with a Mach 3 supersonic nozzle. **Figure 2(a)** shows the atomization test for the suspension liquid (ethylene glycol), **Figure 2(b)** is the image of the initial plasma plume before addition of the (H₂) in the sheath gas and **Figure 2(c)** shows the injected suspension exiting at the plasma plume during deposition.

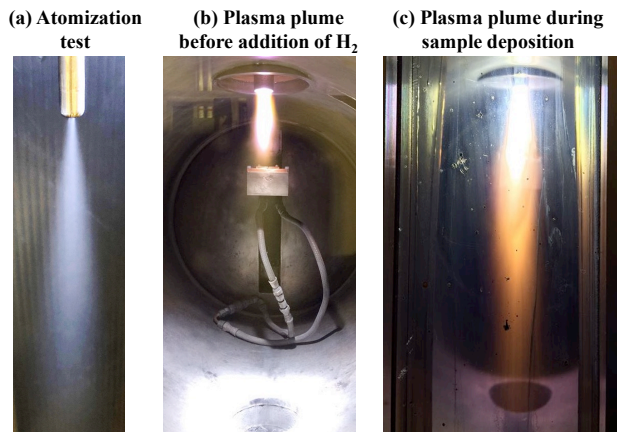


Fig. 2. Pictures of the SPS system.

The substrates were discs of diameter 12 mm, with a thickness of 2 mm and were grid blasted prior to the installation in the water-cooled sample holder. Before the deposition of the coatings, the substrates were pre-heated for several cycles with each pre-treatment cycle lasting 4 seconds. The coating materials were prepared by blending ZrO₂ powder (particle size 0 – 45 μm, supplied by Inframat[®] Corporation, USA) and B₄C powder (1 – 7 μm, supplied by Atlantic Equipment Engineers (AEE), USA) in a molar ratio of 2:1 with an overall mass of 10g and added to 100 ml of the suspension liquid. In this study, the suspension liquids selected for comparison purposes were

ethylene glycol, mineral oil, and hexadecane. The homogenous powder was sprayed through the SPS system onto titanium or cast iron substrate. **Table 1** provides a summary that describes the spraying parameters in detail.

Table 1. Plasma parameters used to synthesize the coating materials.

Property	Samples (Run#)			
	A3	A7	A8	A12
Plasma Power (kW)	48.4	50.4	50.8	52.5
Suspension liquid	Mineral oil	Mineral oil	Hexadecane	Ethylene glycol
Substrate material	Titanium	Titanium	Titanium	Cast iron
Pre-heating (cycles)	35	35	35	25
Deposition (cycles)	40	80	40	80

Atomization gas (Ar: 10 SLPM), central gas (Ar: 21 SLPM), sheath gas (Ar: 78, H₂: 6.5 and N₂: 22 SLPM); reactor pressure = 16 kPa; spraying distance = 11 cm; suspension feed rate = 3 mL/min.

After plasma deposition, the samples were weighed, rinsed in ethanol. For comparison purposes, the starting powders were characterized by X-ray diffraction (XRD) analysis as well as the plasma synthesized samples to measure their phase compositions. The samples were then submerged in an ultrasonic bath for 5 min in order to get a rapid test to assess the coating quality and its cohesiveness and also to assess its good adhesion to the substrate.

3. Results and Discussion

As predicted from the FactSage thermodynamic software [4], a reaction took place between the precursor powder particles in the plasma. The coating could not be destroyed or spalled off after 5 min exposure to an ultrasonic bath in ethanol. Numerous phases including the targeted ZrB₂ were identified. The coating exhibited uniform distribution of fine particles, and ZrB₂ was detected in every coating as confirmed by XRD analysis. In addition, the ZrC phase was observed as a by-product of the reaction, which tends to decrease when an excess of B₄C is introduced into the powder precursors during preparation. Multiple ZrO₂ phases from monoclinic to cubic as well as tetragonal crystal structures have also been observed. The same phases were found by other authors regarding plasma spraying of ZrO₂ and B₄C dry powders, where the addition of 5 to 30-wt.% of B₄C was investigated [5].

While investigating the effect of the suspension liquid on the reaction products, similar XRD patterns were observed for the same suspension liquid used, as shown in **Figure 3**. Although there was a slight variation in the intensity of the XRD signal, the difference was due to the difference in deposition cycles applied between the samples (40 versus 80 cycles), and this is a good indication of the reproducibility of the method. In the XRD patterns, an intense peak at 42° [20]-angle observed alongside two other peaks at 25° and 33° provide evidence for the presence of ZrB₂ in the coating material. The consecutive

intense peaks observed at 28°, 30° and 34° [2θ]-angles signify the presence of ZrO₂ (baddeleyite), ZrO₂ (tazheranite) and ZrC respectively.

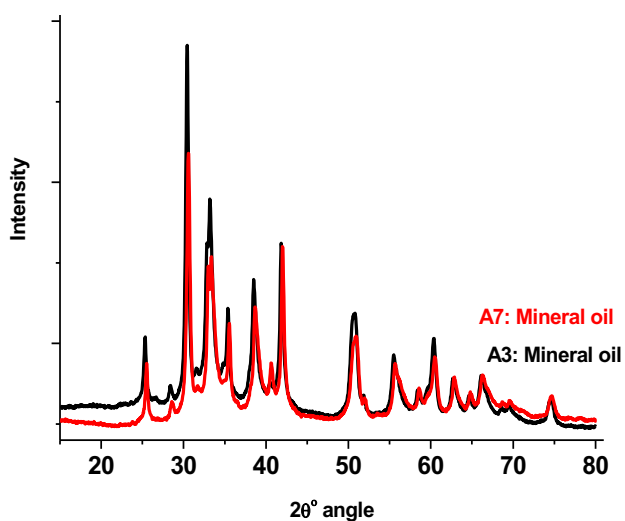


Fig. 3. XRD patterns for samples synthesized using the same suspension liquid (mineral oil).

It was observed that using different suspension liquids produces different phases especially when the intensity of these three peaks at 28°, 30° and 34° [2θ]-angles are considered. This is exemplified in **Figure 4**, which compares the composition of two samples prepared using mineral oil or hexadecane.

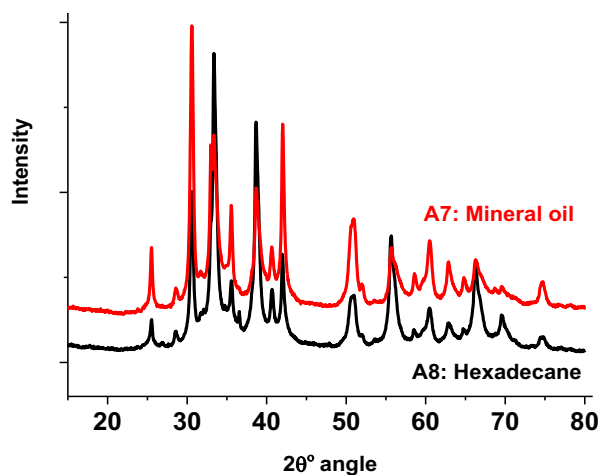


Fig. 4 Comparing XRD patterns of samples synthesized using mineral oil and hexadecane.

This implies that in both XRD patterns, ZrB₂, ZrO₂ and ZrC are some of the major phases identified in the samples. **Figure 5** shows a major contrast between coatings prepared using ethylene glycol and mineral oil, which indicate a variation in the phases produced (ZrB₂, ZrO₂ and ZrC), among others. In order to simplify the Rietveld analysis results, all the various phases of ZrO₂ were summed up and are presented as ZrO₂ even if it is not the exact phase per se. These phases include monoclinic (M),

tetragonal (T), and cubic (C) crystal structures. For example, since ZrB is associated with the ZrB₂ phase, it has been compiled as ZrB₂. Similarly, ZrC having different phases which appear during the analysis are all summed up as ZrC. A summary of their compositions is provided in **Table 2**.

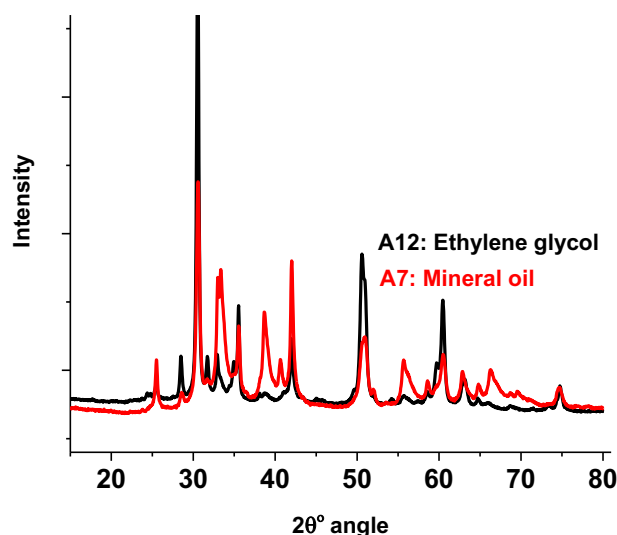


Fig. 5. XRD patterns of samples prepared using mineral oil and ethylene glycol.

Table 2 provides a rough estimate of the phases found in the plasma-synthesized coating materials by Rietveld quantitative analysis (RQA), with the major phases derived from **Figures 3, 4 and 5**.

Table 2. Estimated phases in the plasma-synthesized coatings by Rietveld quantitative analysis.

Sample	Suspension liquid	Composition (%)		
		ZrB ₂	ZrO ₂	ZrC
A3	Mineral oil	22.5	41.5	36.0
A7	Mineral oil	22.0	38.5	39.5
A8	Hexadecane	13.0	24.5	62.5
A12	Ethylene glycol	13.5	81.5	5.0

Since the target phase was ZrB₂, these findings indicate that mineral oil is a better suspension liquid under the current testing condition. In addition, ethylene glycol shows promising results because it minimizes the production of ZrC, and with an excess of B₄C and a diminution of its size, a higher percentage of ZrO₂ can be converted to ZrB₂.

On the other hand, data provided in **Table 3** confirm that the number of deposition cycles is linearly proportional to the coating thickness, for all the suspension liquids used, except the sample prepared using hexadecane, which makes the plasma synthesis method generally reliable.

Table 3. Measured thickness of the coatings

Property	Sample (Run#)			
	A3	A7	A8	A12
Suspension liquid	Mineral oil		Hexadecane	Ethylene glycol
Deposition (cycles)	40	80	40	80
Coating thickness (μm)	90	104	59	114

SEM imaging revealed dense splats of coatings on the substrates. **Figure 6** shows a typical secondary electron image of the coatings prepared using mineral oil and is representative of the observations made for the other coatings as well. From the EDX elemental mapping of the same sample shown in **Figure 7**, uniform dispersion of the three major phases identified by XRD analysis (i.e., ZrB_2 , ZrO_2 and ZrC) can be observed from the widespread presence of Zr, O and C in the coating.

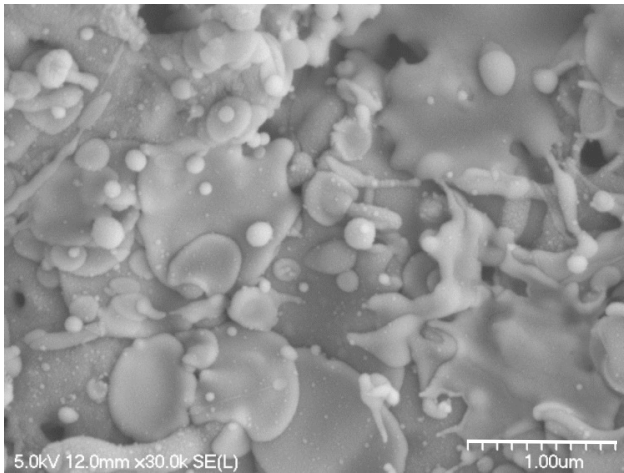


Fig. 6. SEM image of the ZrB_2 -rich coating deposited on titanium substrate in mineral oil suspension A7.

In order to increase the material's toughness as well as to adapt the expansion coefficient of the ZrB_2 -based coating, one strategy is to vary the composition of the coating material with the inclusion of metal phases and ceramics, which are resistant to liquid aluminum. SPS technology has been used in association with plasma reactive spraying to get access to this composition flexibility. It has been shown that the coating quality depends on the nature of the suspension liquid [9].

4. Conclusion

In this work, we report the successful deposition of ZrB_2 on metallic substrates through suspension plasma-spray technology. XRD analysis revealed the presence of ZrB_2 as the target phase, among other measured phases. More investigations are underway to decrease or eliminate the ZrC and ZrO_2 phases from the reaction products.

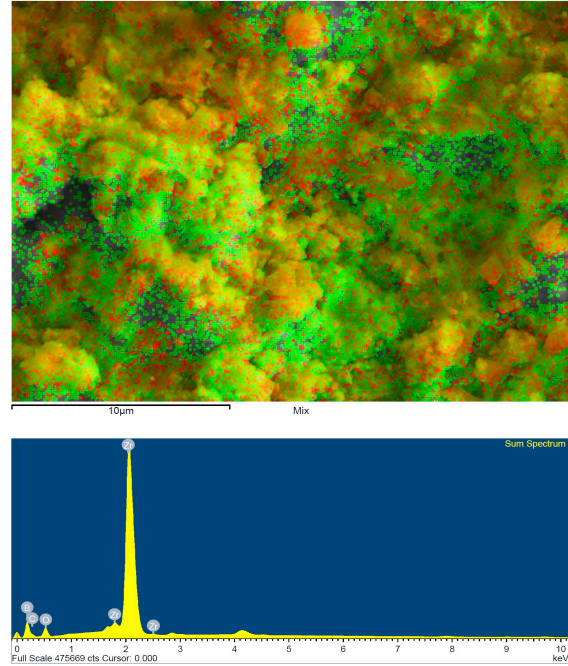


Fig. 7. SEM imaging with EDX elemental mapping of the coating on titania substrate (Run #A7) Green is Zr-rich, Orange is B-rich Blue is O-rich and red is C-rich.

5. Acknowledgements

The authors wish thank ALCOA, Centre québécois de recherche et de développement de l'aluminium (CQRDA), MITACS, Natural Sciences and Engineering Research Council of Canada (NSERC), and Pyrotek Inc., for their financial support.

6. References

- [1] R. Loehman, E. Corral, H.P. Dumm, P. Kotula, and R. Tandon, Sandia Report, Sandia National Laboratories, USA, p.10, (2006).
- [2] Y. Wang. *Surface Engineering*, **15**, 3 (1999).
- [3] Q. Wang, W.J. Wang, H.J. Liu, and C.L. Zeng, *Surface and Coatings Technology*, **313**, 129 (2017).
- [4] C. W. Bale, E. Bélisle, P. Chartrand, S. A. Decterov, G. Eriksson, A.E. Gheribi, K. Hack, I. H. Jung, Y. B. Kang, J. Melançon, A. D. Pelton, S. Petersen, C. Robelin, J. Sangster and M-A. Van Ende, *FactSage Thermochemical Software and Databases, 2010-2016*, *Calphad*, **54**, 35 (2016).
- [5] P.K.P. Rupa, P. Sharma, R.M. Mohanty, and K. Balasubramanian, *Journal of Thermal Spray Technology*, **19**, 4 (2010).
- [6] E.Y. Jung, J.H. Kim, S.H. Jung, and S.C. Choi, *Journal of Alloys and Compounds*, **538**, 164 (2012).
- [7] F. Gitzhofer, E. Bouyer, and M.I. Boulos, *Journal of Materials, Journal of the Minerals, Metals & Materials Society*, **49**, 58 (1997).
- [8] M.I. Boulos, *Journal Thermal Spray Technology*, **1**, 33 (1992).
- [9] É. Darthout, G. Laduye; F. Gitzhofer, *Journal of Thermal Spray Technology*, **25**, 1264 (2016).